Bidirectional Active EMC Filter for Industrial Power Converters

Bernhard Wunsch[1], Stanislav Skibin[1], Ville Forsstrom[2]
[1]ABB Corporate Research, 5405 Baden, Switzerland
[2]ABB Oy Drives, 00381 Helsinki, Finland
E-Mail: bernhard.wunsch@ch.abb.com, stanislav.skibin@ch.abb.com,
ville.forsstrom@fi.abb.com
URL: https://abb.com

Keywords

«EMC/EMI», «active filter», «power converter», «Adjustable speed drive», «Filtering», «Parasitic inductance»

Abstract

Size and cost of EMC filters of power converters can be reduced using active circuits. In this work we demonstrate the filter performance of a bidirectional active EMC filter in an industrial 75kW power converter driving a motor. The active filter is bidirectional since it suppresses EMC noise on either side of the filter. The voltage noise source on the grid side stems from magnetic coupling between input and output of the converter. For a purely passive EMC filter, grid side noise needs to be filtered by large inductors. We show that the active filter which is based on current sensing and current injection strongly reduces the magnetic filter components required.

Introduction

Switch mode power supplies emit high frequency noise towards the grid. The emitted EMC noise is limited by international EMC norms like CISPR 11 [1] or product norms like EN61800-3 [2]. EMC filters are placed at the input of the converters in order to comply with these norms. These filters contribute significantly to the cost and size of the converter. One way to reduce the size of the passive filter elements is to improve their filter performance using HF-active circuits. However, despite of many publications on active and hybrid EMC filters [3]-[11] their use in high power converters especially with AC-input is still challenging. Depending on the characteristic impedances on power converter or grid side, different topologies of the active circuit are preferred [7].

In this work we discuss an additional important selection criterion for the active circuit topology, namely bidirectionality, as explained in the following. While in a simplified EMC analysis of power converters it is often assumed that the EMC noise source is placed on the converter side of the EMC filter, parasitic couplings can lead to induced voltages at the grid side of the EMC filter, see Fig. 2. Such a mechanism is analyzed in detail in [12] for the example of an industrial motor drive connected between the 3-phase AC-grid and a three-phase motor, a similar setup is used here. Fig. 1 shows a photo of the setup consisting of a 75 kW power converter driving a motor. As shown in the subfigure (b) input and output cables are located next to each other thus causing a magnetic coupling between the noisy currents on the motor cable and current on the supply cable on the grid side, which is required to have low EMC noise.

This input-output coupling can be represented by an induced voltage source that drives current from the grid side towards the EMC filter see Fig. 2. Since the EMC filter needs to suppress noise on either side of the filter, EMC noise is filtered much more efficiently by inductive filter elements than by shunt capacitors.

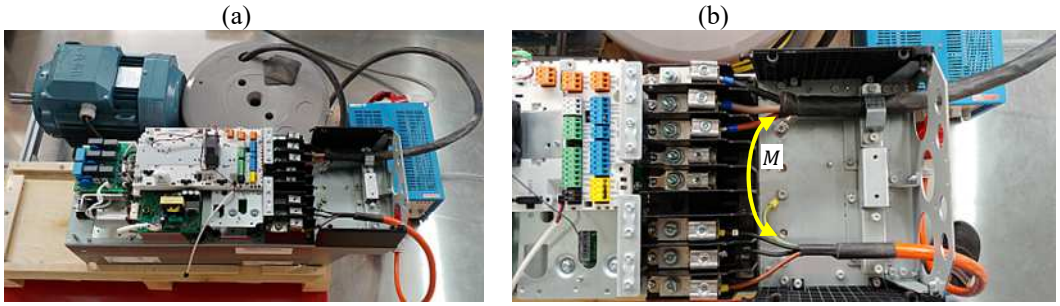

Fig. 1 (a) Photo of the EMC setup consisting of LISN, AC-AC power converter, motor cable and motor. (b) The grid side cable is connected close to and in parallel to the motor side cable which introduces a large input-output coupling bypassing the passive EMC filter.

Based on the requirement on bidirectionality of the EMC filter, we select the topology of the active circuit to be based on a current-controlled current-source. In this publication we demonstrate the active EMC filter in a 75 kW power converter driving a motor [12]. The active filter allows strong reduction of magnetic components of a purely passive filter, and it is also immune to the main parasitic bypass degrading the passive filter. Compared to previous work on active EMC filter, the novelty here is the high power of the drive (75 kW) and the focus on bidirectionality of the active filter. In the next section, we discuss the operation principle of the active circuit. Then we introduce the active board and show the performance of the active EMC filter (AEF) in the power converter. In the final section we conclude this work.

Operation principle of active circuit

In this section we summarize key features of active circuits used for EMC filtering based on a simple single line equivalent representation of noise source and victim. For the power converter studied in the next chapter, such a single line equivalent circuit has been derived for the common mode (CM) noise in [12].

Active circuits used for filtering realize controlled sources and can be classified by the quantity that is sensed and the quantity that is controlled. Both sensed and output quantity can be either current or voltage which results in four possible combinations, like current-controlled current-source etc. Additionally, the circuits can be distinguished as feed backward or feed forward depending on the relative location of the sensing part and actuation part of the circuit. If the sensing occurs closer to the noise source than the actuation, then the circuit is called feed forward type and if the sensing occurs closer to the victim than the actuation, then the circuit is of backward type [6], [7].

In active circuits based on voltage actuation the injection mechanism is realized by an inductor on the power line between source and victim. For large power converters the power lines are realized by thick cables or large busbars so that the inductors are bulky and costly. Therefore, an active circuit based on current actuation was chosen in this work, where the controlled source is placed on a shunt connection between noise source and victim.

A circuit based on voltage-sensing current-actuation behaves as a controlled shunt impedance. This topology can effectively filter noise from the converter, if the controlled shunt impedance is smaller than the converter output impedance and the victim impedance. It can be argued that this topology is the easiest to implement since there is no need of inductors for sensing or actuation [13]. However, the low shunt impedance will be ineffective and in fact even harmful for a voltage noise source on the victim/grid side. Therefore, such an active filter is not bidirectional.

Therefore, the selected topology uses current-sensing current-actuation in either feedback or feedforward topology. Both topologies enable a bidirectional filtering of voltage noise sources and can

be understood as an effective multiplication of the source impedance by the current gain [3]. The operation principle is visualized in Fig. 2 for ideal controlled current sources. The LISN current is driven by the noise source U_{src} of the converter and the induced noise source U_{ind} on the grid side. Both sources are suppressed by the same total impedance Z_{tot} consisting of the series connection of the LISN impedance Z_{LISN} and the input impedance Z_{in} of the converter. The active circuit increases the input impedance of the converter by a factor depending on the current gain and topology.

$$I_{LISN} = \frac{U_{ind}+U_{src}}{Z_{LISN}+Z_{in}};\ Z_{in} = \begin{cases} Z_{src}\,(1+F) & \text{feedback} \\ Z_{src}/(1-F) & \text{feed-forward} \end{cases} \tag{1}$$

In principle both topologies are suited as bidirectional filter. For good filter performance a high gain |F|≫1 is required for the feedback configuration whereas an accurate gain of F→1 is required for the feedforward configuration. After first tests with both configurations, we selected the feedback configuration since we found the accurate control of both magnitude and phase required for the feedforward topology more challenging. The same topology has been assessed in previous works [3]-[10].

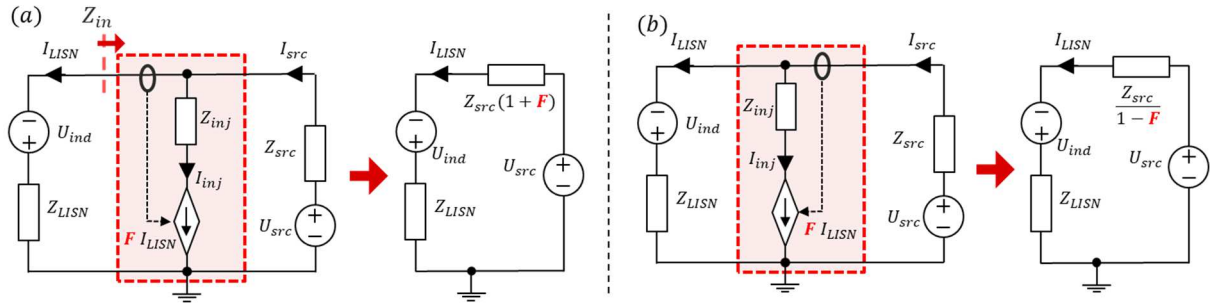

Fig. 2 The active circuit based on current-sensing current-actuation leads to a multiplication of the source impedance [3], see (1). (a) Feed-backward configuration has multiplication factor $Z_{in} = Z_{src}(1+F)$. (b) Feed-forward configuration has multiplication factor $Z_{in} = Z_{src}/(1-F)$.

Active EMC Filter Board and the test setup

The AEF board is used to reduce the CM filter of conducted EMC noise in a high-power motor drive. The active circuit board realizes a current-controlled current-source $I_{AEF} = F\ I_{LISN}$ where F labels the unitless current amplification. This topology has been selected since it enables bidirectional noise filtering as discussed above.

A photo of the board together with its schematic circuit diagram is shown in Fig. 3. The controlled current-source is realized by a series combination of a current transformer and a Howland current source, which also includes a push-pull stage to increase the output current capabilities, see [4] for a similar design. The current amplification F of the active filter is set by the current transformer load resistor R_{CT} , its turn number N_2, as well as by the three impedances of the Howland current source, namely the input resistance R_{in}, the feedback resistance R_f, and the sense resistance R_{sense}, see Fig. 3:

$$I_{AEF} = \frac{R_{CT}}{N_2}\frac{R_f}{R_{in}\,R_{sense}}\ I_{LISN}. \tag{2}$$

Beside of the Howland current source, the AEF board contains a power supply unit (PSU) and the injection circuit. The PSU is powered from the local supply (+24 V) and provides the active circuit with a bipolar voltage (±15 V). The injection circuit consists of a Y2 rated capacitor, C_{inj}, and three X2 rated capacitors. The Howland current source is built up around a TI LM7171 voltage feedback OpAmp with Unity-Gain Bandwidth of 200 MHz and specified for ±15 V operation. The push-pull stage uses Diodes Inc. ZDT6753 complimentary medium power transistors which are rated for 100 V

collector-emitter voltage and 2 A continuous current. The current transformer showed in Fig. 4 (a) is built up using 10 turns of the secondary winding around a Vacuumschmelze T60004-L2050-W626 core. The detailed analysis of the active filter board and its hardware realization is beyond the scope of the current article and will be published elsewhere.

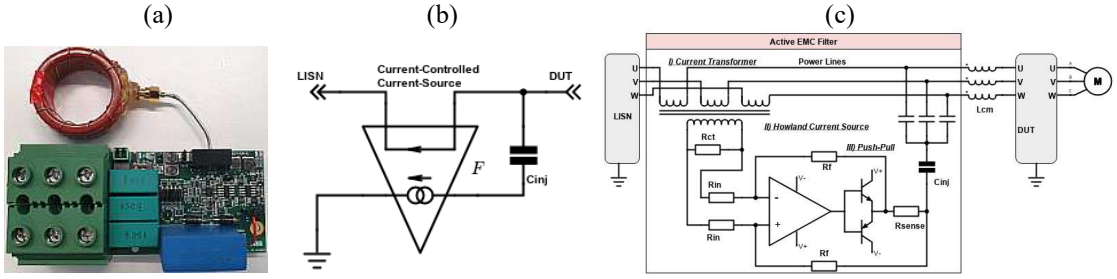

Fig. 3: AEF board prototype (a), its operational principle with respect to the filtering of CM noise (b) and a simplified circuit diagram (c). Due to the active filtering the common mode choke can be strongly reduced. A schematic of the power converter is shown in Fig. 5 (a).

Fig. 4 AEF board installation inside the test setup on Fig.1 (a)

The developed AEF board has been tested in a setup shown in Fig. 1 (a). The footprint of the designed AEF board allows its installation inside the motor drive for the normal operation (see Fig. 4). However, in the tests below, the board is mounted externally to ensure equal conditions in the benchmark of the active filter versus passive one.

The schematic of the test setup is shown in Fig. 5 and has been discussed in detail in [12]. The 75 kW motor drive is connected on the grid side to a 32 A, 3-phase LISN and the load consists of 30 m long 3-phase shielded motor cable with 16 mm^2 wire cross-section and 15 kW motor. The coupling between motor and grid cables is captured by coupled loop inductances L_{p1}, L_{p3} with a coupling parameter k_{13}. This parasitic coupling introduces the induced common mode voltage U_{ind} on the grid side of the filter (see Fig. 2). The induced voltage $U_{ind} = j\,\omega\,M\,i_3$ with $M = k_{13}\sqrt{L_{p1}L_{p2}}$ denoting the mutual inductance and i_3 the motor side current, see Fig. 5 (b).

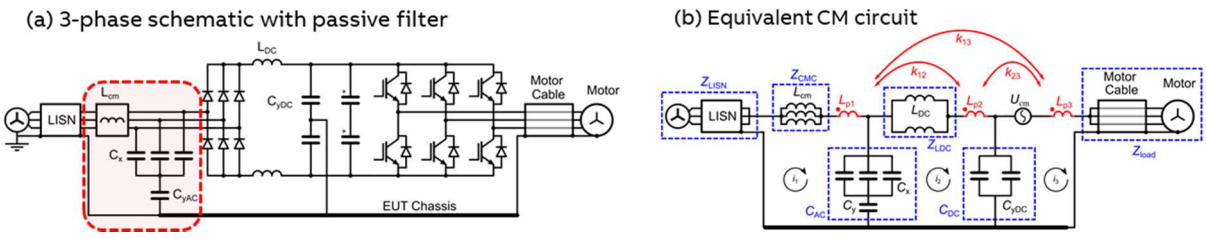

Fig. 5 (a) Simplified schematic of the EMC setup shown in Fig. 4. The EMC input filter is highlighted. Objective of the active board is to reduce the size of the common mode inductance L_{CM} using the idea

of impedance multiplication discussed in section 2. (b) Corresponding common mode circuit. Details can be found in [12].

Test setup and measurement results

Benchmark 1: Influence of cross coupling between motor and grid cables on emitted EMC noise

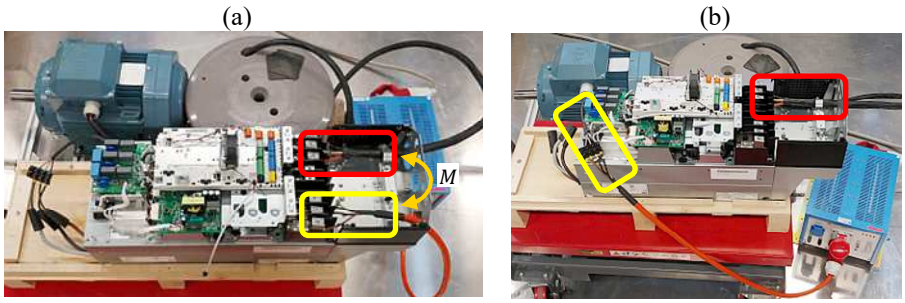

Fig. 6: Test setup for the evaluation of the cross-coupling effect. (a) – original cable connection where motor and grid cable are attached on same side and in parallel, corresponding to large mutual inductance M, (b) – attachment of the grid cable at the back of the drive opposite to the motor cable, thus minimizing the coupling.

In the first test, we quantify the importance of the magnetic input-output coupling which introduces the grid side noise source thus requiring a bi-directional EMC filter. The coupling can be strongly reduced by modifying the connection of the AC grid cable to the backside of the converter opposite to the motor cable connection as shown in Fig. 6 (b). Note that the same components are present but only the parasitic mutual coupling k_{13} is changed. Fig. 6 (a) shows the original cable connection where motor and grid cables are attached to the same side of the motor drive and run in parallel which maximizes the magnetic coupling. Fig. 6 (b) shows a modified setup where the grid cable is attached at the back of the drive, avoiding cable cross-coupling. In this test, the motor drive is attached to a 15 kW asynchronous motor via a shielded 30 m long motor cable with 16 mm^2 wire cross-section. The measured CM-noise without CM-choke on the grid side for the setups shown in Fig. 6 are shown by the red and green curve in Fig. 7. The blue curve in Fig. 7 shows the EMC noise in presence of input-output coupling but with the CM-chokes added see Fig. 8 (a).

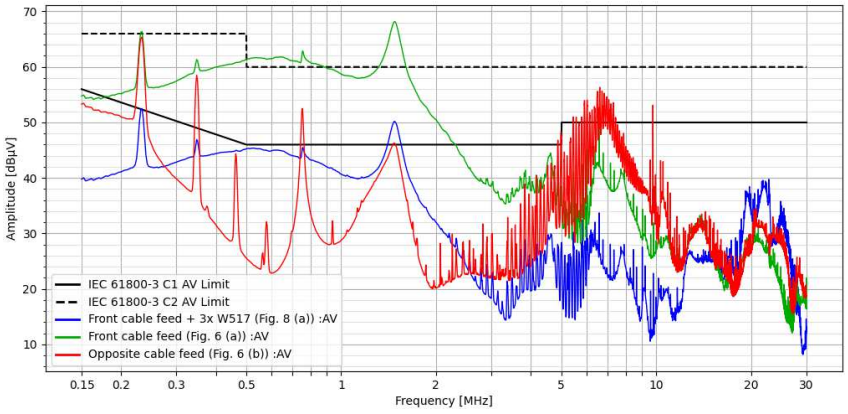

Fig. 7: Various measurements of EMC noise (CM noise using average detector). Red and green curves illustrate the impact of input-output coupling (two different connections of grid side cable see Fig. 6) without CM-choke. Blue curve shows EMC filtering of blue curve when CM-inductance is added as in Fig. 8 (a).

The following conclusions can be drawn from the results shown in Fig. 7:

- The EMC noise in the range 300 kHz – 4 MHz is dominated by the cross-coupling effect between motor and grid cables. The difference between green and red curves shown in Fig. 7 is caused by the noise source U_{ind} caused by the magnetic coupling of input and output cables.
- To comply with the EMC in presence of cross-coupling corresponding to the original cable connection shown in Fig. 6 (a), a large common mode inductor consisting of 3 × Vacuumschmelze (VAC) W517 cores is placed on the grid side of the inverter as shown in Fig. 8 (a). EMC measurements of this setup are shown by blue curve in Fig. 7.

Benchmark 2: Application of the bi-directional active filter within motor drive

As discussed in previous sections, the bi-directional AEF efficiently filters HF noise stemming from noise sources located on DUT and/or grid sides (U_{src} and U_{ind} from the equivalent circuit on Fig. 2). In this benchmark, we evaluate the performance of the AEF using a 30 m motor cable with 16 mm^2 wire cross-section and an asynchronous 15 kW motor and compare it to the conventional passive filter, consisting of three VAC W517 cores (see Fig. 7 (a)). The designed AEF board has also been successfully tested in our lab using different combinations of motors and cables which will not be shown here because of the lack of space

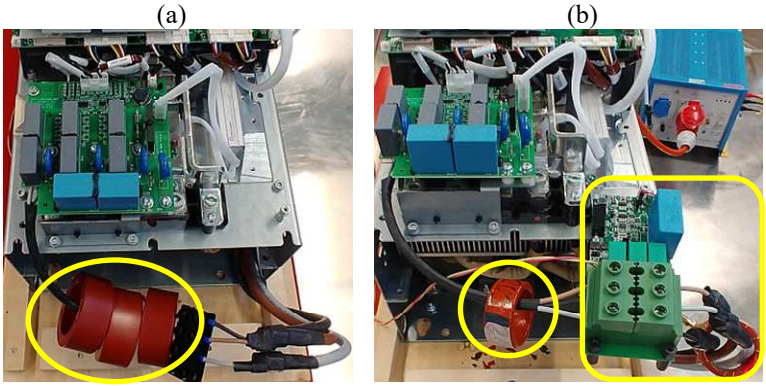

Fig. 8: Test setup for the evaluation of the AEF performance: using passive filter (a), using active filter (b). The common choke is strongly reduced when using the active circuit board.

The AEF board is connected as shown in Fig. 8 (b) to ensure similar cross-coupling effects for passive and active EMC filtering. Motor and grid cables are connected on the same side as shown in Fig. 7 (a). In presence of the active filter the common mode choke can be reduced to a single VAC W625 core on the DUT side due to the impedance multiplication effect from the active circuit, see (1).

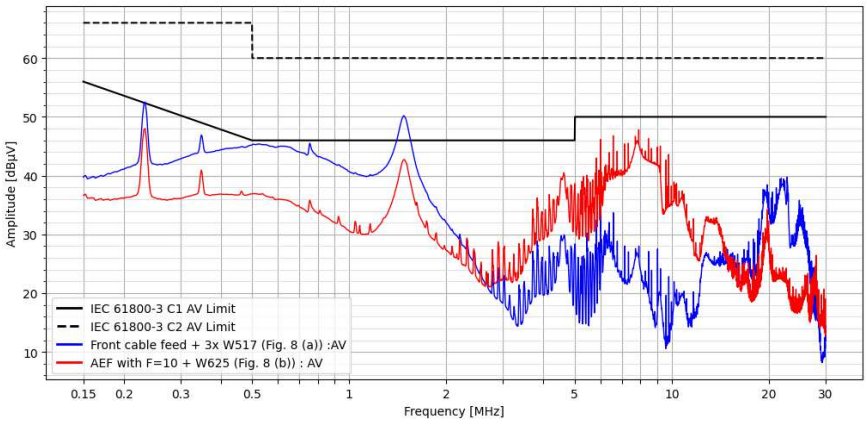

Fig. 9: Measured AV EMC noise of the passive and active (F=10) filters in a setup with 30 m long motor cable

In the Fig. 9, measurement results of the AEF board with a single VAC W625 on the DUT side vs. pure passive filter with 3 × VAC W517 cores are shown. Motor and grid cables are connected on the same side as shown in Fig. 7 (a). The designed AEF performs significantly better than the pure passive filter in the range up to few MHz with a much smaller CM choke. The CM noise even complies with the C1 limit of EN 61800-3. The filter performance of the currently designed board degrades in the range above few MHz .

Conclusion

In this paper, a successful application of the Active EMC Filter (AEF) in a power inverter driving a motor has been presented, leading to a strong reduction of magnetic filter components. It has been shown that the coupling between input and output cables introduces a voltage noise source on the AC-gird side of the EMC filter so that bi-directionality of the active filter is essential. Therefore, a current-sensing current-actuation active filter topology (both feed backward and feed forward) has been selected. In the scope of this paper, we showed an implementation of the above-mentioned topology and its successful application in an industrial motor drive for realistic operation conditions. The designed Active EMC Filter showed very good performance up to few MHz which is the typical "problem" range for the high-power motor drive applications, providing significant cost cut (70% reduction of expensive Nanocrystalline cores) in the EMC filter design.

References

[1] CISPR 11-Industrial Scientific and Medical Equipment-Radio-Frequency Disturbance Characteristics-Limits and Methods of Measurement. CISPR 11:2015|IEC Webstore|Electromagnetic Compatibility, EMC, Smart City. Available online: https:// webstore.iec.ch/publication/22643 (accessed on 11 March 2021).

[2] EN/IEC 61800-3, Ed. 3.0, Adjustable Speed Electrical Power Drive Systems–Part 3: EMC Requirements and Specific Test Methods, 2017. IEC 61800-3:2017|IEC Webstore|Electromagnetic Compatibility, EMC, Smart City, Pump, Motor, Water Management. Available online: https://webstore.iec.ch/publication/31003 (accessed on 11 March 2021).

[3] W. Chen, X. Yang, and Z. Wang, "A novel hybrid common-mode EMI filter with active impedance multiplication," *IEEE Trans. Ind. Electron.*, vol. 58, no. 5, pp. 1826–1834, 2011.

[4] S. Wang, Y. Y. Maillet, F. Wang, D. Boroyevich, and R. Burgos, "Investigation of hybrid EMI filters for common-mode EMI suppression in a motor drive system," *IEEE Trans. Power Electron.*, vol. 25, no. 4, pp. 1034–1045, 2010.

[5] Y. Chu, S. Wang, and Q. Wang, "Modeling and Stability Analysis of Active/Hybrid Common-Mode EMI Filters for DC/DC Power Converters," *IEEE Trans. Power Electron.*, vol. 31, no. 9, pp. 6254–6263, 2016.

[6] N. K. Poon, J. C. P. Liu, C. K. Tse, and M. H. Pong, "Techniques for input ripple current cancellation: Classification and implementation," *PESC Rec. - IEEE Annu. Power Electron. Spec. Conf.*, vol. 2, no. 6, pp. 940–945, 2000.

[7] Y. C. Son and S. K. Sul, "Generalization of active filters for EMI reduction and harmonics compensation," *IEEE Trans. Ind. Appl.*, vol. 42, no. 2, pp. 545–551, 2006.

[8] M. L. Heldwein, H. Ertl, J. Biela, and J. W. Kolar, "Implementation of a transformerless common-mode active filter for offline converter systems," IEEE Trans. Ind. Electron., vol. 57, no. 5, pp. 1772–1786, 2010.

[9] Amaducci, "Design of a wide bandwidth active filter for common mode EMI suppression in automotive systems," IEEE Int. Symp. Electromagn. Compat., pp. 612–618, 2017.

[10] E. Mazzola, F. Grassi, and A. Amaducci, "Enhanced Circuit Model for Insertion Loss Prediction of Active EMI Filters Considering Non-ideal Parameters," in *2020 International Symposium on Electromagnetic Compatibility - EMC EUROPE*, Sep. 2020, pp. 1–5.

[11] S. Jeong, D. Shin, and J. Kim, "A Transformer-Isolated Common-Mode Active EMI Filter Without Additional Components on Power Lines," *IEEE Trans. Power Electron.*, vol. 34, no. 3, pp. 2244–2257, 2019.

[12] B. Wunsch, S. Skibin, V. Forsström, and I. Stevanovic, “EMC Component Modeling and System-Level Simulations of Power Converters: AC Motor Drives”, *Energies*, vol. 14, no. 6, p. 1568, 2021.

[13] M. L. Heldwein, J. Biela, H. Ertl, T. Nussbaumer, and J. W. Kolar, “Novel Three-Phase CM/DM Conducted Emission Separator,” *IEEE Trans. Ind. Electron.*, vol. 56, no. 9, pp. 3693–3703, Sep. 2009.